Spectroscopic verification of zinc absorption and distribution in the desert plant *Prosopis juliflora-velutina* (velvet mesquite) treated with ZnO nanoparticles

J.A. Hernandez-Viezcas[a], H. Castillo-Michel[b], A.D. Servin[a], J.R. Peralta-Videa[a], J.L. Gardea-Torresdey[a,b,*]

[a] Chemistry Department, The University of Texas at El Paso, 500 West University Ave., El Paso, TX 79968, United States
[b] Environmental Science and Engineering PhD Program, The University of Texas at El Paso, 500 West University Ave., El Paso, TX 79968, United States

ABSTRACT

The impact of metal nanoparticles (NPs) on biological systems, especially plants, is still not well understood. The aim of this research was to determine the effects of zinc oxide (ZnO) NPs in velvet mesquite (*Prosopis juliflora-velutina*). Mesquite seedlings were grown for 15 days in hydroponics with ZnO NPs (10 nm) at concentrations varying from 500 to 4000 mg L^{-1}. Zinc concentrations in roots, stems and leaves were determined by inductively coupled plasma optical emission spectroscopy (ICP-OES). Plant stress was examined by the specific activity of catalase (CAT) and ascorbate peroxidase (APOX); while the biotransformation of ZnO NPs and Zn distribution in tissues was determined by X-ray absorption spectroscopy (XAS) and micro X-ray fluorescence (μXRF), respectively. ICP-OES results showed that Zn concentrations in tissues (2102 ± 87, 1135 ± 56, and 628 ± 130 mg kg^{-1} d wt in roots, stems, and leaves, respectively) were found at 2000 mg ZnO NPs L^{-1}. Stress tests showed that ZnO NPs increased CAT in roots, stems, and leaves, while APOX increased only in stems and leaves. XANES spectra demonstrated that ZnO NPs were not present in mesquite tissues, while Zn was found as Zn(II), resembling the spectra of Zn(NO$_3$)$_2$. The μXRF analysis confirmed the presence of Zn in the vascular system of roots and leaves in ZnO NP treated plants.

© 2011 Published by Elsevier B.V.

1. Introduction

Increasing production and use of nano-sized materials have raised concerns about their possible impacts on environmental and human health. Due to their small size, nanoparticles (NPs) display unique properties that are used in nanotechnology [1]. Nanotechnology is growing very fast and it has been estimated that will contribute $1 trillion to the U.S. economy by 2015 [2]. As with any technological advance, the applications of nanotechnology could bring significant benefits but also great risk in terms of the environmental and human health.

Zinc oxide (ZnO) NPs have unique optical and electrical properties which can be used in a variety of applications such as coatings for solar cells [3], gas sensors [4], UV absorbing [5], and as antibiotics [6]. ZnO NPs are included in a list of 14 representative manufactured nanomaterials (NM) for testing by the Organization for Economic Cooperation and Development [7]. These NMs are already being produced, sold, commercially used, and likely have entered soil, water and air. As part of the first trophic level, plants should be tested to determine their response and possible role in the fate and transport of NPs. Risk assessment and nanotoxicological studies have been made on a few model and crop plants [8–10]; however, to our knowledge, nothing is known about the potential effects of NM on wild desert plants. Since they have acquired special characteristics to survive in harsh environments [11], it is hypothesized that plants from desert ecosystems will respond differently to NPs than plants in other ecosystems. Importantly, desert plants such as mesquite (*Prosopis juliflora-velutina*) improve soil structure and properties, and play an important role in the stability and conservation of other species [12].

Plants have special mechanisms to remove or inactivate reactive oxygen species (ROS) such as H$_2$O$_2$, OH$^-$, and O$_2$$^-$ radicals that are byproducts of naturally occurring reactions. However, excess ROS can result in protein breakdown, lipid peroxidation in membranes, and DNA injury [13]. Previous studies have shown that heavy metals increased the activity of the antioxidant enzymes catalase (CAT) and ascorbate peroxidase (APOX) in plants [14]. However, there is lack of information on the effects of NPs upon ROS molecules. Lin et al. [15] reported a decrease in the superoxide dismutase activity (SOD) of Arabidopsis cells exposed to multiwalled carbon nanotubes (MWCNTs). In a study with rice cells treated with MWCNTs at 20 mg L, a significant time dependent induction was observed [16]. In order to obtain an insight about the metabolic state of mesquite in response to ZnO NPs, stress was quantified by the spe-

* Corresponding author at: Chemistry Department, The University of Texas at El Paso, 500 West University Ave., El Paso, TX 79968, United States.
Tel.: +1 915 747 5359.
E-mail address: jgardea@utep.edu (J.L. Gardea-Torresdey).

cific activity of the antioxidant enzymes CAT and APOX. Micro X-ray fluorescence (μXRF) technique has been successfully used to investigate the distribution and speciation of Zn in Arabidopsis plants [17]. In the present study, this technique was used to determine Zn speciation and distribution in mesquite plants treated with ZnO NPs.

The objectives of this investigation were to evaluate the uptake and phytotoxicity of ZnO NPs on *P. juliflora-velutina*, the oxidation state and distribution of Zn in tissues and the effect of ZnO NPs on the activity of anti-ROS molecules. μXRF, X-ray absorption spectroscopy (XAS), and inductively coupled plasma-optical emission spectroscopy (ICP-OES) were used as analytical techniques.

2. Materials and methods

2.1. Preparation of ZnO suspensions

The hexagonal ZnO NPs (10 nm) were purchased from Meliorum Technologies (Rochester, NY). Suspensions were prepared in a Hoagland modified nutrient solution previously described in the literature [18]. Zinc was present as a micronutrient in the Hoagland solution at a concentration of 0.37 μM. Dilutions were performed in order to obtain the desired ZnO NPs concentration (0, 500, 1000, 2000, and 4000 mg L^{-1}) mixtures were stirred for 5 min and later sonicated for 30 min in an ice bath. All suspensions were freshly prepared before each experimental setup and adjusted to pH 5.8. To determine the NP aggregation, suspensions at concentrations varying from 500 to 4000 were prepared in the Hoagland modified nutrient solution. These suspensions were sonicated as previously described and pH adjusted to 5.8. After seven days under constant bubbling, the aggregation was determined using a light scattering VARIAN model PDDLS/Coolbatch 90T dynamic light scattering (DLS) with Precision Deconvolve^{32} software (Bellingham, MA.)

2.2. Seed germination

Mesquite seeds were purchased from Granite Seeds (Lehi, UT). Seeds were presoaked for thirty minutes in 4% NaClO$_4$ solution, rinsed 5 times with sterilized Millipore Water (MPW) and left overnight in sterilized MPW. Seeds were then placed in paper towels soaked with an antibiotic–antimycotic solution (A5955, Sigma, St. Louis, MO) to prevent fungal and bacterial contamination. After four days in the dark, plants were exposed to light for one more day and transferred to 200 mL jars containing a suspension of nanoparticles diluted in the nutrient solution. The seedlings were suspended in stock jars using polyurethane foam and plastic micropipettes on the top; therefore, only the roots were in contact with the nanoparticle suspension. Seedlings were allowed to grow for fifteen days at room temperature on a 16-h photoperiod (two 34 W Phillips lamps). During this period, the solution level was maintained nearly constant by adding MPW every day. Triplicate sets of 40 plants/jar (200 mL) were set, for a total of 600 plants per experiment. Jars were continually aerated with aquarium pumps to provide oxygen and to maintain the NPs in suspension. Zinc ions were not included as treatments due to the very low solubility of the nanoparticles. For the zinc oxide the solubility was about 8 mg L^{-1} for the 4000 mg L^{-1} treatment [11].

2.3. Quantification of Zn in dry plant tissues

For metal quantification, all plants were washed with 0.01 M HNO$_3$ and MPW to remove the NPs stuck on root surface. Subsequently, the plants were cut in roots, stems, and leaves and dried at 60 °C for 4 days. Next, samples were microwave digested using a CEM microwave (CEM Mars$_x$, Mathews, NC). Samples treated with

ZnO NPs were digested using 3 mL plasma pure HNO$_3$ (SCP Science, New York) and diluted to 25 mL using MPW following the USEPA 3051 method (1200 W, 5 min ramping to 175 for 10 min at a pressure of 350PSI). Concentrations in plant parts were determined using ICP-OES. Certified standard reference materials (NIST-SRF 1570) of metals and metalloids (Metuchen, NJ) were used for calibration and quality assurance/quality control. In addition, an external certified standard of each element was used after every 10 samples to monitor the matrix effect on the analytes.

2.4. CAT/APOX assay

After 15 days of exposure to the NPs treatments, the plants were washed with 0.01 M HNO$_3$ and MPW to remove any external contaminant. From every treatment, extracts of root, stem, and leaves of three plants were used to determine the activity of CAT according to Gallego et al. [19] with minor variations. For each treatment, a ratio of 10% (w/v) of root, stem or leaf samples was extracted with phosphate buffer (25 mM KH$_2$PO$_4$ at pH 7.4) by using a glass–glass homogenizer. Extracts were centrifuged for 5 min at 4 °C and 10,000 rpm in a refrigerated centrifuge (Eppendorf AG bench centrifuge 5417 R, Hamburg, Germany). Supernatants were transferred to microcentrifuge tubes for the assay [14]. A sample of 990 μL of 10 mM H$_2$O$_2$ was placed in a quartz cuvette and an aliquot of 10 μL of the sample was added to obtain a final volume of 1 mL. The mixture was mixed by hand (shaken three times) and the absorbance at 240 nm was recorded in a Perkin Elmer Lambda 14 UV/Vis Spectrometer (single-beam mode, Perkin-Elmer, Uberlinger, Germany). The absorbance values were obtained from the first linear section of slope between 0.5 and 1 min. The extinction coefficient for H$_2$O$_2$ was set at 36.1 mM^{-1} cm^{-1}. The amount of protein for CAT/APOX was determined according to the Bradford method with serum albumin as standard [20].

APOX activity was evaluated according to Murguia et al. [21] with minor modifications. Extract of leaves were prepared as described above. The supernatant was separated after centrifugation. A volume of 886 μL of 0.1 M KH$_2$PO$_4$ buffer at pH 7.4, 10 μL of 17 mM H$_2$O$_2$, 100 μL of the sample, and 4 μL of a 25 mM solution of ascorbate were placed in a quartz cuvette and mixed. The absorbance was recorded at 265 nm in a Perkin Elmer Lambda 14 UV/Vis Spectrometer. The absorbance was recorded as described above and the extinction coefficient for H$_2$O$_2$ was experimentally set at 36.1 mM^{-1} cm^{-1}.

2.5. MicroXRF data acquisition

Roots of mesquite plants treated with 1000 mg ZnO NPs L^{-1} were washed twice with 0.01 M HNO$_3$ and three times with DI water to eliminate any excess of NPs on the root surface. Roots were then sectioned in a Minotome plus cryostat (Triangle Biomedical Sciences, Durham, NC). Root samples were dissected 0.5 mm up from the root tip. Samples were frozen and embedded into specimen holders enclosed by Tissue Tek (Sakura Finetek USA, Inc., Torrance, CA). Samples were sectioned axially at 30 μm and 100 μm thick and mounted onto Kapton tape. Leaves were immersed in liquid nitrogen for 45 min and lyophilized at −53 °C and 0.140 mbar pressure for 3 days (Labcono FreeZone 4.5, Kansas City, MO). Micro-XRF mapping of the distribution of Zn and other elements in the leaves and roots was performed at beamline 10.3.2 of the Advanced Light Source, Lawrence Berkeley National Laboratory (ALS, Berkeley, CA) [22]. Freeze-dried leaf and root sections were fixed on a x–y translation stage, cooled down to −20 °C to prevent radiation damage, and scanned under a micro focused beam. Maps were recorded using a 5 μm × 5 μm beam and a 100–120 ms dwell time. The fluorescence yield was measured at an incident energy of 10 keV using a seven-element germanium (Ge) solid-
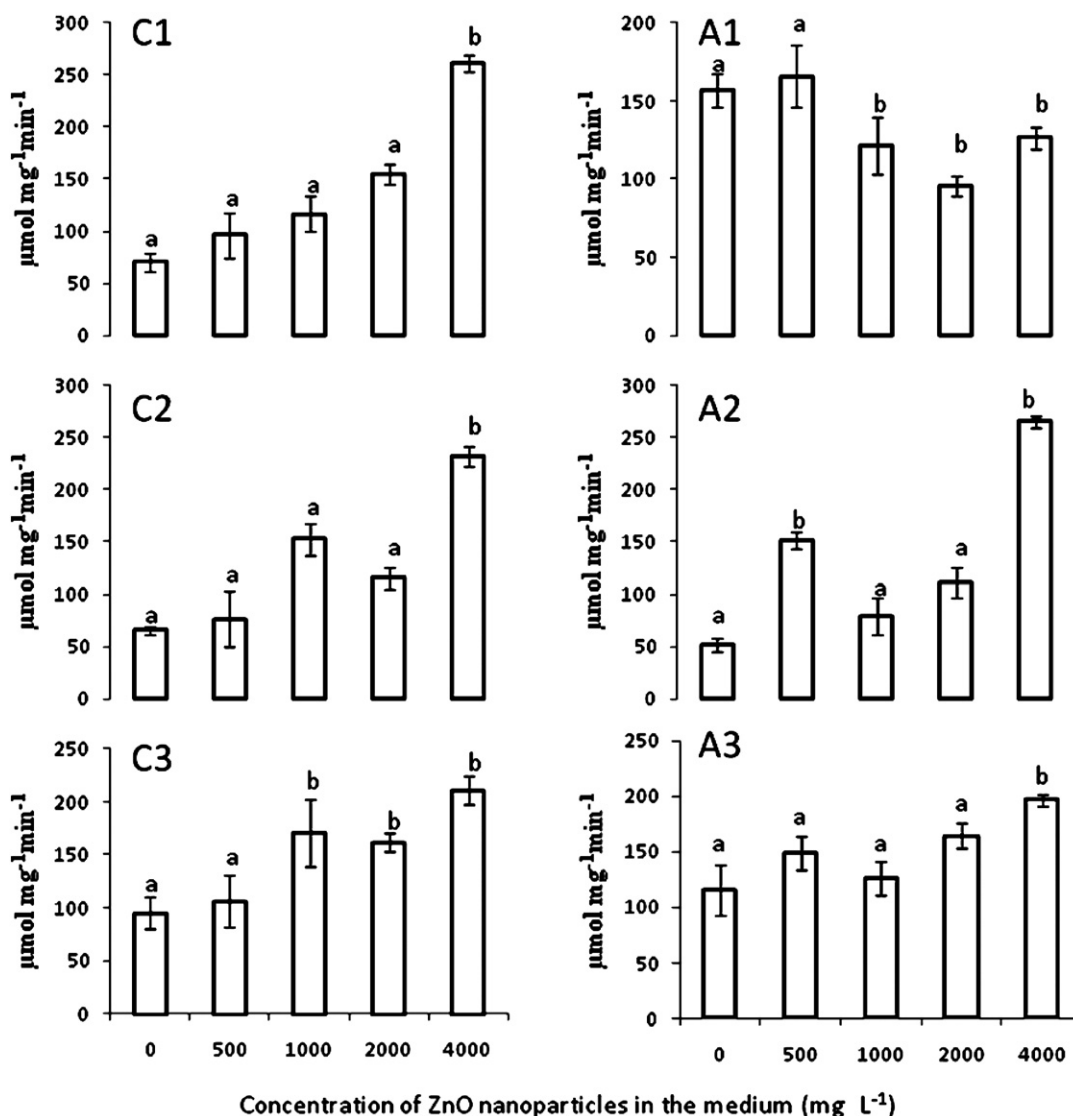
Fig. 1. CAT (C) and APOX (A) specific activity in (1) roots, (2) stems, and (3) leaves of mesquite plants grown in hydroponics for 15 days under ZnO NPs treatment. Values are means ± SE. [a,b]Significant differences at $p \leq 0.05$ between treatments for the same enzyme/tissue.

state detector and normalized by I_0 and the dwell time. Several bright and diffused points were selected from the XRF maps for Zn K-edge X-ray absorption near edge structure (XANES) analysis. XANES spectra were processed using a suite of programs available at beamline 10.3.2. Briefly, spectra were energy-calibrated with respect to a Zn foil (inflection point at 9658.76 eV) and the pre-edge background was subtracted and normalized using a linear pre-edge.

2.6. Statistics

The data reported for Zn uptake and CAT/APOX activity are averages of three replicates ± standard errors (SE). A one-way ANOVA test was performed followed by Tukey-HSD (honestly significant difference) test performed with the statistical package SPSS Version 12.0 (SPSS, Chicago, IL, USA). In all cases the statistical significance is based on a probability of $p < 0.05$.

2.7. XAS data acquisition

Plants from the 4000 mg ZnO L^{-1} treatment were cleaned with 4% NaClO solution, followed by rinsing with MPW. Roots, stems and

leaves were immersed in liquid nitrogen for 45 min and lyophilized on a freeze dryer at −53 °C and 0.140 mbar pressure for 3 days (Labcono FreeZone 4.5, Kansas City, MO). After that, samples were homogenized in a mortar, loaded in aluminum sample holders, and covered with Kapton tape.

The XAS spectra were collected on beamline 7-3 at Stanford Synchrotron Radiation Light Source (SSRL, Palo Alto, CA). During data collection, the synchrotron radiation accelerator had a ring storage energy of 3 GeV and a beam current of 50–100 mA. Zn-K edge was collected using a Canberra 29-element germanium detector and Si(2 2 0) ψ 90 monochromator.

Zinc foil was used to calibrate sample spectra. Fluorescence and transmission mode were used for collecting all sample spectra and model compounds, respectively, at room temperature. Zinc nitrate, and ZnO NPs were used as model compounds. The WinXAS software [23] was used to analyze the data. Edge energies from individual spectra were calibrated using the edge energy from the internal zinc foil (9659 eV). First and second degree derivatives of the inflection point of the metal foil were used to calibrate the sample spectrum, and a polynomial fitting subtraction was done in order to remove background. A first and fourth degree polynomial were used on the pre-edge and post edge region of the spectrum, respectively.

Speciation of Zn was determined based on the XANES spectra from model compounds [24].

3. Results and discussion

3.1. CAT/APOX results

The effects of ZnO NPs on CAT and APOX specific activity are shown in Fig. 1. As seen in this figure, at all concentrations ZnO NPs increased CAT activity in roots (C1), stems (C2), and leaves (C3) (Fig. 1). It seems that APOX activity changed in the whole plant by the mere presence of the ZnO NPs in roots. In addition, APOX response to ZnO NPs was different in each plant organ. As seen in Fig. 1A1, the NP concentrations higher than $500 \, mg \, L^{-1}$ produced a reduction of APOX activity. However, APOX increased in the above ground plant parts at all ZnO NP concentrations, though in leaves the increase reached statistical significance only at $4000 \, mg \, L^{-1}$ (Fig. 1A1 and A2). A similar response was reported by Cuypers et al. [25] in common beans (*Phaseolus vulgaris*). These researchers reported that the mere contact of Zn with roots ($50 \, \mu M$) temporary reduced APOX activity in roots, but increased the activity of this enzyme in leaves. The plants were left in the NP suspensions for another 15 days (30 days in total), and even at the high NP concentrations, mesquite plants showed no visible signs of stress like chlorosis, necrosis, wilting or stunting.

3.2. Zn accumulation

The ICP-OES result from the certified reference material and external standards showed recoveries for zinc of 99%. Absorption of Zn by mesquite plants from the ZnO NP treatments is shown in Table 1. As seen in this table, at $500 \, mg \, ZnO \, NPs \, L^{-1}$ in the medium, the concentration of Zn in roots was about $3800 \, mg \, kg^{-1}$ d wt;

Table 1

Zinc concentration in roots, stems, and leaves of mesquite plants treated for 15 days in hydroponics with ZnO nanoparticles. Results are means ± SE. One-way ANOVA and Tukey's test were used to determine statistical significance. Means with same letter are statistically equals at $p \leq 0.05$.

Treatment (mg ZnO NPs L^{-1})	Dry biomass (mg Zn kg^{-1})		
	Root	Stem	Leaf
Control	93 ± 25a	59 ± 2a	71 ± 9a
500	3837 ± 161b	1061 ± 70b	423 ± 77b
1000	2516 ± 210b	949 ± 33b	450 ± 17b
2000	2102 ± 87b	1135 ± 56b	628 ± 130b
4000	2017 ± 122b	1113 ± 96b	400 ± 42b

however, in plants treated with $1000–4000 \, mg \, ZnO \, NPs \, L^{-1}$, concentrations of Zn in roots varied from 2500 to $2000 \, mg \, Zn \, kg^{-1}$ d wt. These results could be determined by the aggregations of the NPs in the nutrient solution (Fig. 2). As seen in this figure, the average diameter of the particles at $500 \, mg \, L^{-1}$ (Fig. 2B) was about 990 nm. Furthermore, at $500 \, mg \, L^{-1}$ there were particles with a diameter $\leq 100 \, nm$ resulting in more NPs and Zn ions available for plant uptake. Fig. 2 also shows that at concentrations of 1000, 2000 and $4000 \, mg \, NPs \, L^{-1}$, the NPs formed larger aggregates (Fig. 2C–E), being the largest at $4000 \, mg \, L^{-1}$. As previously reported [26], in aqueous environment NPs tend to attract each other and form aggregates. This process affects the mobility of NPs and can determine their final sink. Franklin et al. [27] reported that ZnO at $100 \, mg \, L^{-1}$ showed agglomeration resulting in flock formations of different sizes (nm to μm).

Bioconcentration factors in roots (metal in roots/metal in medium) had indices of 7.6, 2.5, 1.0, and 0.5 for 500, 1000, 2000, and $4000 \, mg \, L^{-1}$ treatments. This reduction in the bioconcentration factors suggests that Zn in roots came from absorption, not from

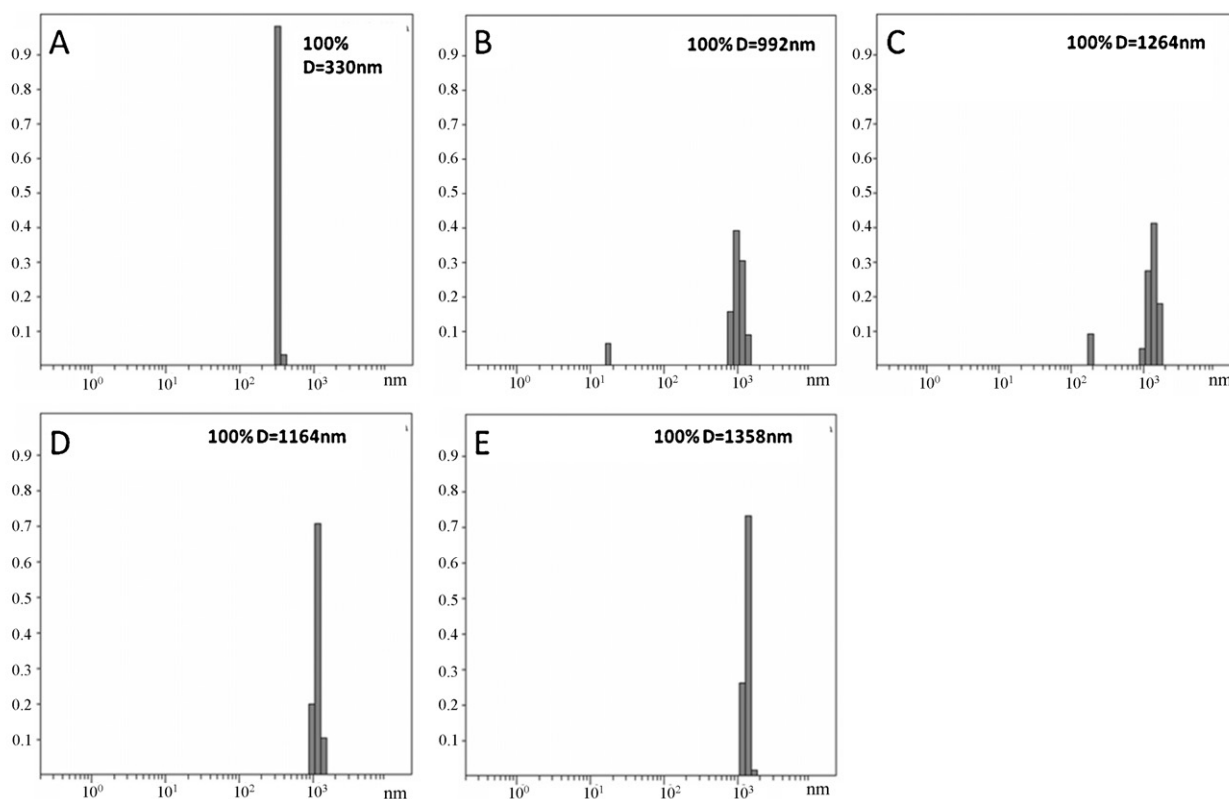**Fig. 2.** Dynamic light scattering determination of particle sizes in (A) nutrient solution, (B–E) nutrient solution with $500 \, mg \, L^{-1}$, $1000 \, mg \, L^{-1}$, $2000 \, mg \, L^{-1}$, and $4000 \, mg \, L^{-1}$, of ZnO NPs, respectively. The X axis shows particle diameter and the Y axis the normalized counts. The average particle diameter in nanometers is shown in the upper right corner.
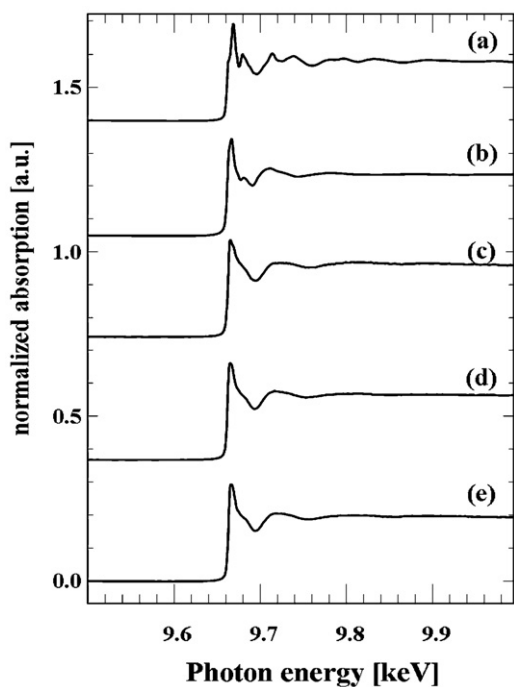
Fig. 3. XANES K-edge spectra (9.659 keV) of the model compounds (a) ZnO NPs, and (b) $Zn(NO_3)_2$, and spectra of (c) leaves, (d) stems, and (e) roots of mesquite germinated in 4000 mg ZnO NPs L^{-1}.

possible adsorption of the ZnO NPs on root surface. The data also suggest that mesquite plant did not transport much of the Zn concentrated in roots to the shoots. In all cases the translocation factors from roots to shoots were <1. It has been reported that Zn is required by more than 200 enzymes [28], and many of these enzymes are used by plants in roots to synthesize essential molecules [29]. Lin and Xing [30] reported that translocation factors of Zn from root to shoot in *Lolium perenne* were very low under ZnO NP treatments, since the NPs were maintained in the apoplast and protoplast of the root endodermis and stele.

So far it is not possible to differentiate how much of the Zn in roots came from Zn dissociated from the NPs. However, de la Rosa et al. [11] have reported that the concentration of Zn ions in the supernatant of 500, 1000, 2000, and 4000 mg ZnO NPs L^{-1} solutions were 8, 32, 35, and 8 mg Zn L^{-1}, respectively, which suggests that most of the Zn in tissues came from the nanoparticles. More studies are needed to elucidate this issue.

3.3. XAS results

Fig. 3 shows bulk XANES spectra of the model (pure) compounds (a) ZnO NPs and (b) $Zn(NO_3)_2$ as well as spectra of (c) leaves, (d) stems, and (e) roots of mesquite grown with ZnO NPs at 4000 mg L^{-1}. By comparing the XANES spectra obtained from mesquite plant tissues with spectra of the model compounds, it can be seen that in all mesquite tissues Zn was not present as ZnO NPs. The data could suggest that ZnO NPs were biotransformed on/in root surface and transported as Zn(II) from roots to leaves. This response differs slightly from the response found in mesquite treated with non-coated $Ni(OH)_2$ NPs. Non-coated $Ni(OH)_2$ NPs, were only partially biotransformed in roots but fully biotransformed in stems to a Ni–organic acid compounds [31]. In the present study, spectra showed that Zn was found as Zn(II) and resembled the spectra of $Zn(NO_3)_2$. This means that Zn was probably coordinated in the same manner as zinc nitrate (Fig. 3). These results concurred with those obtained by Lopez-Moreno et al. [24]
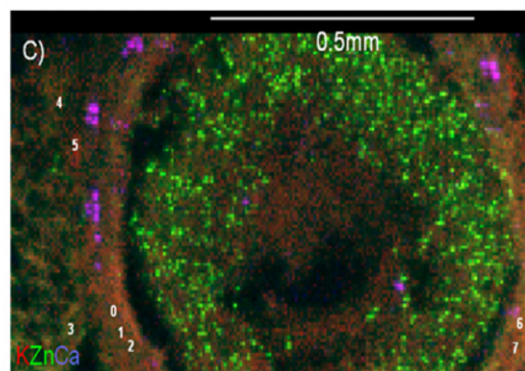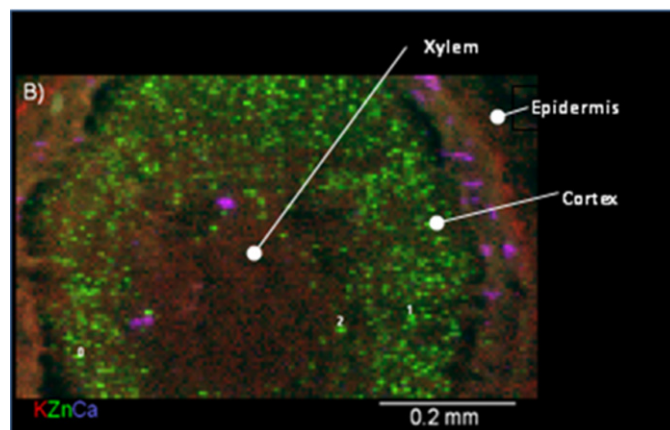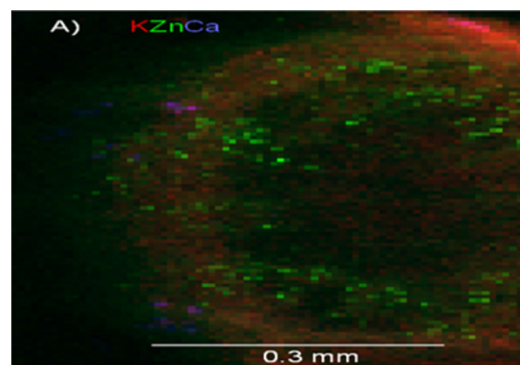

Fig. 4. Tricolour micro-XRF images of the cross sections of (A) mesquite root control (sample of 100 μm of thickness); (B) and (C) two different mesquite roots samples treated with 1000 mg L^{-1} (sample of 30 μm of thickness). Red colour stands for potassium, green for zinc, and purple for calcium. In (B) and (C), bright spots are labelled with numbers from 0 to 2 and diffused spots with numbers 0 to 7. (For interpretation of the references to colour in this figure legend, the reader is referred to the web version of the article.)

in soybean, where they found that within the tissues Zn was in the oxidation state of Zn(II) but not present as ZnO NPs. Further studies need to be done in order to clarify the possible uptake and biotransformation mechanisms of NPs in plants.

3.4. μXFR results

Fig. 4A shows a tricolour XRF map (potassium, zinc and calcium (K, Zn, Ca)) for control roots from plants grown in nanoparticle-free nutrient solution. The thickness of the control root was 100 μm in order to obtain higher Zn fluorescence signal and improve the quality of the map. Fig. 4B and C shows the tricolour XRF maps of root samples treated with 1000 mg ZnO NPs L^{-1} (samples 30 μm thick). Although the thickness of NP treated samples was lower than the
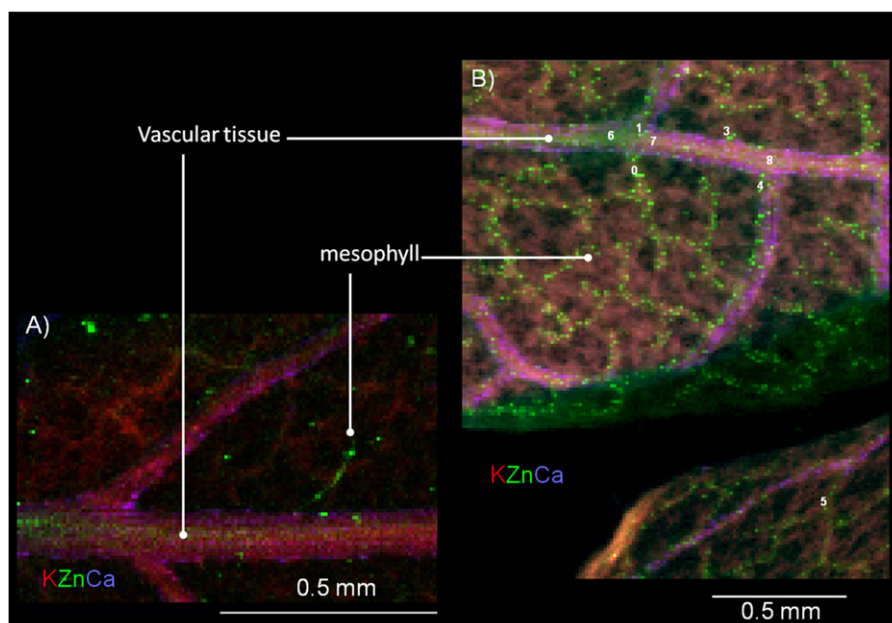
Fig. 5. Tricolour micro-XRF images of (A) mesquite leaves control and (B) mesquite leaves treated with 1000 mg L^{-1}. Red colour stands for potassium, green for zinc, and purple for calcium. In (B), bright spots are labelled with numbers from 0 to 5 and diffused spots with numbers 6 to 8. (For interpretation of the references to colour in this figure legend, the reader is referred to the web version of the article.)

thickness of control samples, they showed a greater and brighter number of spots (Fig. 4B and C) compared to control (Fig. 4A). This suggests that most of the Zn shown in Fig. 4B and C was from the ZnO NPs. Fig. 5 shows the XRF maps of the leaf control (Fig. 5A) and leaf treated with 1000 mg ZnO NPs L^{-1} (Fig. 5B). As shown in Fig. 5B, leaves treated with ZnO NPs had more Zn in the vascular system compared to the control (Fig. 5A). In the XRF maps, bright and diffuse fluorescence Zn spots were observed on several regions of the leaves and roots treated with ZnO NPs. K-edge μXANES was then performed on bright and diffuse spots of leaf and root μXRF maps.

Fig. 6. XANES region K-edge spectra of the ZnO NPs, and average spectra of the leaf and root diffuse and bright spots.

A total of 9 bright spots were selected: 3 marked from 0 to 2 in the root (Fig. 4B) and 6, marked 0 to 5 in the leaf (Fig. 5B). Pertaining to diffuse spots, a total of 11 spots were selected: 8 marked from 0 to 7 in root (Fig. 4C) and 3 marked from 6 to 8 in leaf (Fig. 5B). Fig. 6 compares the XANES spectra of ZnO NPs (pure compound) and the μXANES of the bright green spots and the diffuse spots from the root and leaf. The bright leaf and root spots spectra had almost identical spectral signature (Fig. 6, lower spectra). These forms of Zn compounds are different from the forms obtained from the diffuse spectra. The diffuse root spots have a white line feature shifted to higher energy (9667 eV) and shorter period of the first oscillation above 9692 eV (Fig. 6). Also, the amplitude of the first oscillation for both diffuse root and leaf spots was different indicating diverse Zn coordination environments. It is hypothesized that the shorter period in the spectra of the diffuse root possibly suggests an octahedral geometry. Different Zn ligands such as organic acids (malate, citrate and oxalate) and Zn phosphate have been identified by linear combination fittings to reference samples in the Zn accumulator plant *Arabidopsis halleri* [17]. However, there were no clear findings from the XANES studies in mesquite. The organic acid content of the mesquite plants should be further studied in order to identify possible Zn organic ligands to use as references for XANES analysis.
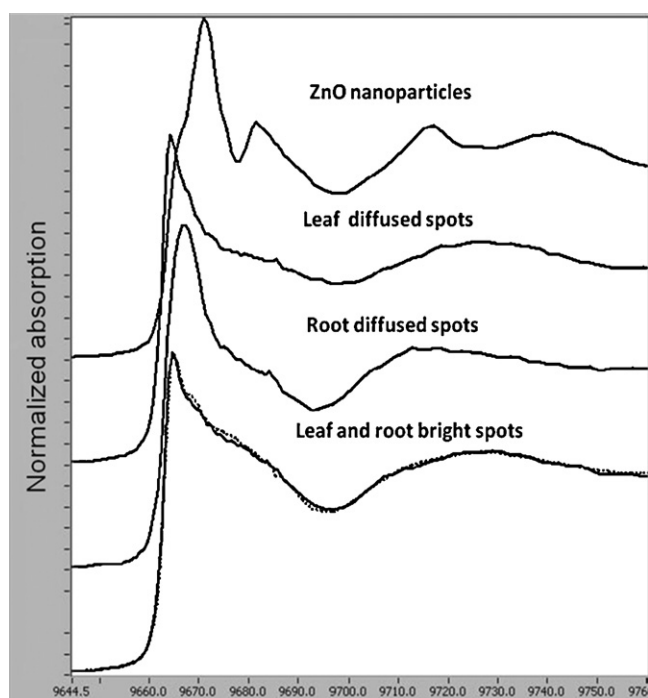
4. Conclusion

The results of this study indicate that mesquite plants (*P. juliflora-velutina*) absorbed Zn from the NPs treatments as demonstrated by ICP OES. The reduction in the bioconcentration factors and the μXRF images suggest that Zn in roots came from absorption, not from possible adsorption of the ZnO NPs on root surface. Biochemical assays showed that the ZnO increased the specific activity of stress enzymes CAT in root, stem and leaves and APOX only in stem and leaves. However, mesquite plants showed no chlorosis, necrosis, stunting or wilting, even after 30 days of treatment, suggesting that this desert plant may display some tolerance to ZnO NPs and to the Zn ion released from these particles.

The XAS study showed no evidence of the presence of the ZnO NPs within tissues. Spectra show that Zn was found as Zn(II)

and resembled the spectra of $Zn(NO_3)_2$. This means that Zn was probably coordinated in the same manner as zinc nitrate. The XANES analysis of the bright and diffused spots in μXRF maps of the root and leaf corroborated the biotransformation of the ZnO NPs and suggests the forms of Zn compounds in bright spots are different from the forms obtained from the diffuse spectra. This study demonstrated the importance of the use of μXRF and μXANES in the study of Zn accumulation by plants. The μXAS analyses are complementary to the bulk XAS studies as they allow observing changes in speciation with respect to localization.

References

[1] E. Hood, Nanotechnology, Looking as we leap, Environ. Health Perspect. 112 (2004) a740–a749.
[2] M.C. Roco, W. Bainbridge, Societal Implications of Nanoscience and Nanotechnology, Springer, Boston, 2001.
[3] J. Yoo, J. Lee, S. Kim, K. Yoon, J. Park, S.K. Dhungel, B. Karunagaran, D. Mangalaraj, J. Yi, High transmittance and low resistive ZnO:Al films for thin film solar cells, Thin Solid Films 480 (2005) 213–217.
[4] H. Xu, X. Liu, D. Cui, M. Li, M. Jiang, A novel method for improving the performance of ZnO gas sensors, Sens. Actuators B: Chem. 114 (2006) 301–307.
[5] T. Sato, T. Katakura, S. Yin, T. Fujimoto, S. Yabe, Synthesis, UV-shielding properties of calcia-doped CeO_2 nanoparticles coated with amorphous silica, Solid State Ionics 172 (2004) 377–382.
[6] N. Jones, R. Binata, T. Koodali, M. Adhar, Antibacterial activity of ZnO nanoparticle suspensions on a broad spectrum of microorganisms, FEMS Microbiol. Lett. 279 (2007) 71–76.
[7] A. Kahru, H.C. Dubourguier, From ecotoxicology to nanoecotoxicology, Toxicology 269 (2–3) (2009) 105–119.
[8] M.L. Lopez-Moreno, G. de la Rosa, J.A. Hernandez-Viezcas, J.R. Peralta-Videa, J.L. Gardea-Torresdey, X-ray absorption spectroscopy (XAS) corroboration of the uptake and storage of CeO_2 nanoparticles and assessment of their differential toxicity in four edible plant species, J. Agric. Food Chem. 58 (2010) 3689–3693.
[9] W.M. Lee, Y.J. An, H. Yoon, H.S. Kweon, Toxicity and bioavailability of copper nanoparticles to the terrestrial plants mung bean (*Phaseolus radiatus*) and wheat (*Triticum aestivum*): plant agar test for water-insoluble nanoparticles, Environ. Toxicol. Chem. 27 (2008) 1915–1921.
[10] R. Barrena, E. Casals, J. Colón, X. Font, A. Sánchez, V. Puntes, Evaluation of the ecotoxicity of model nanoparticles, Chemosphere 75 (2009) 850–857.
[11] de la Rosa, Lopez-Moreno, Hernandez-Viezcas, Peralta-Videa, Gardea-Torresdey, Toxicity and biotransformation of ZnO nanoparticles in the desert plants *Prosopis juliflora-velutina*, *Salsola tragus* and *Parkinsonia florida*, Int. J. Nanotechnol., in press.
[12] S. Luna-Suárez, M.L. Luna-Guido, J.T. Frias-Hernández, V. Olalde-Portugal, L. Dendooven, Soil processes as affected by replacement of natural mesquite ecosystem with maize crop, Biol. Fert. Soils 27 (1998) 274–278.
[13] S. Choudhury, S.K. Panda, Induction of oxidative stress and ultrastructural changes in moss *Taxithelium nepalense* (Schwaegr.) both under lead (Pb) and arsenic (As) phytotoxicity, Curr. Sci. 87 (2004) 342–348.
[14] M.L. Lopez, J.R. Peralta-Videa, H. Castillo Michel, A. Martinez-Martinez, M. Duarte-Gardea, J.L. Gardea-Torresdey, Lead toxicity in alfalfa plants exposed to phytohormones and EDTA monitored by peroxidase catalase and amylase activities, Environ. Toxicol. Chem. 26 (2007) 2717–2723.
[15] C. Lin, Y. Fugetsu, F. Watari, Studies on toxicity of multi-walled carbon nanotubes on Arabidopsis T87 suspension cells, J. Hazard. Mater. 170 (2009) 578–583.
[16] X. Tan, C. Lin, B. Fugetsu, Studies on toxicity of multi-walled carbon nanotubes on suspension rice cells, Carbon 45 (2009) 3479–3487.
[17] G. Serret, G. Williams, M-P. Isaure, M.A. Marcus, S.C. Fakra, H. Frerot, S. Pairis, N. Geoffroy, A. Manceau, P. Saumitou-Laprade, Zinc distribution and speciation in *Arabidopsis halleri × Arabidopsis lyrata* progenies presenting various zinc accumulation capacities, New Phytol. 184 (2009) 581–595.
[18] J.R. Peralta-Videa, J.L. Gardea-Torresdey, E. Gomez, K.J. Tiemann, J.G. Parsons, G. Carrillo, Effect of mixed cadmium, copper, nickel and zinc at different pHs upon alfalfa growth and heavy metal uptake, Environ. Pollut. 119 (2002) 291–301.
[19] S.M. Gallego, M.P. Benavides, M.L. Tomaro, Effect of heavy metal ion excess on sunflower leaves: evidence for involvement of oxidative stress, Plant Sci. 121 (1996) 151–159.
[20] N. Kruger, The Protein Protocols Handbook, The Bradford Method for Protein Quantitation Department of Plant Sciences, University of Oxford, UK, 2008.
[21] I. Murguia, D. Tarantino, C. Vannini, M. Bracale, S. Carravieri, C. Soave, *Arabidopsis thaliana* plants overexpressing thylakoidal ascorbate peroxidase show increased resistance to paraquat-induced photooxidative stress and to nitric oxide-induced cell death, Plant J. 38 (2004) 940–953.
[22] M.A. Marcus, A.A. MacDowell, R. Celeste, A. Manceau, H.A. Padmore, R.E. Sublett, Beamline 10.3.2 at ALS: a hard X-ray microprobe for environmental and material sciences, J. Synchrotron Radiat. 11 (2004) 239–247.
[23] T. Ressler, WinXAS: a program for X-ray absorption spectroscopy data analysis under MS-Windows, J. Synchrotron Radiat. 5 (1998) 118–122.
[24] M.L. Lopez-Moreno, G. de la Rosa, J.A. Hernandez-Viezcas, H. Castillo-Michel, C. Botez, J.R. Peralta-Videa, J.L. Gardea-Torresdey, Evidence of the differential biotransformation of ZnO and CeO2 nanoparticles on soybean (*Glycine max*) plants, Environ. Sci. Technol. (2010), doi:10.1021/es903891g.
[25] A. Cuypers, J. Vangronsveld, H. Clijsters, The redox status of plant cells (AsA and GSH) is sensitive to zinc imposed oxidative stress in roots and primary leaves of *Phaseolus vulgaris*, Plant Physiol. Biochem. 39 (2001) 657–664.
[26] K. Chen, M. Elimelech, Aggregation and deposition kinetics of fullerene (C-60) nanoparticles, Langmuir 22 (2006) 10994–11001.
[27] N.J. Franklin, S.C. Rogers, G.E. Apte, G.E. Batley, P.S. Gadd, P.S. Casey, Comparative toxicity of nanoparticulate ZnO, bulk ZnO, and ZnCl2 to a freshwater microalga (*Pseudokirchneriella subcapitata*): the importance of the particle solubility, Environ. Sci. Technol. 41 (2007) 8484–8490.
[28] G. Rayner-Canham, Descriptive Inorganic Chemistry, 2nd ed., Freeman, New York, 1999.
[29] F.B. Salisbury, C.W. Ross, Plant Physiology, 2nd ed., Wadsworth Publishing Company, Belmont, CA, 1978.
[30] D. Lin, B. Xing, Root uptake and phytotoxicity of ZnO nanoparticles, Environ. Sci. Technol. 42 (2008) 5580–5585.
[31] J.G. Parsons, M.L. Lopez, C.M. Gonzalez, J.R. Peralta-Videa, J.L. Gardea-Torresdey, Toxicity and biotransformation of uncoated and coated nickel hydroxide nanoparticles on mesquite plants, Environ. Toxicol. Chem. 29 (2009) 1146–1154.